

THE LUMINOSITY FUNCTION OF ω CENTAURI¹

GUIDO DE MARCHI

European Southern Observatory, Karl-Schwarzschild Strasse 2, D-85748 Garching, Germany; demarchi@eso.org

Received 1998 June 18; accepted 1998 September 14

ABSTRACT

Deep *Hubble Space Telescope* (*HST*) Wide Field Planetary Camera 2 observations of the stellar population in the globular cluster ω Cen (NGC 5139) have been used to measure the luminosity function of main-sequence stars at the low-mass end. Two fields have been investigated, located ~ 4.6 and $\sim 7'$, respectively, away from the cluster center or near the half-light radius of this cluster ($r_{\text{hl}} \simeq 4.8$). The color-magnitude diagrams derived from these data show the cluster main sequence extending to the detection limit at $I \simeq 24$. Information on both color and magnitude is used to build the luminosity functions of main-sequence stars in these fields, and the two independent determinations are found to agree very well with each other within the observational uncertainty. Both functions show a peak in the stellar distribution around $M_I \simeq 9$, followed by a drop at fainter magnitudes well before photometric incompleteness becomes significant, as is typical of other globular clusters observed with the *HST*. This result is at variance with previous claims that the luminosity function of ω Cen stays flat at low masses but is in excellent agreement with recent Near Infrared Camera and Multi-Object Spectrograph observations.

Key words: globular clusters: general — globular clusters: individual (NGC 5139, NGC 6397) — stars: luminosity function, mass function

1. INTRODUCTION

With a total mass of $\sim 3.9 \times 10^6 M_{\odot}$ (Meylan 1987), ω Cen (NGC 5139) is the most massive globular cluster (GC) in the Galaxy. Such a large mass, coupled with the strong anisotropy measured in the velocity dispersion (Meylan 1987), implies that, except probably in the innermost regions, the cluster has not yet reached relaxation through energy equipartition, and therefore the mass function (MF) of main-sequence (MS) stars should still reflect the unperturbed initial mass function (IMF), as no dynamical modifications should have occurred. It is, thus, somewhat surprising that Elson et al. (1995) obtain for ω Cen a luminosity function (LF) that deviates substantially at the low-mass end from that of other clusters with similar metal content. In fact, while low-metallicity clusters such as NGC 6397 (Paresce, De Marchi, & Romaniello 1995; Cool, Piotto, & King 1996), NGC 7078 (De Marchi & Paresce 1995), NGC 7099 (Piotto, Cool, & King 1997), NGC 6254 and NGC 6809 (De Marchi & Paresce 1996), and NGC 6656 (De Marchi & Paresce 1997) all show a LF that reaches a peak at $M_I \simeq 9$ and then drops all the way to the detection limit, the results published by Elson et al. for ω Cen feature a flat LF below $M_I \simeq 8$, with no signs of a drop.

The actual shape of the LF may vary with the location inside the cluster because of dynamical evolution, both internal due to two-body relaxation and external due to the interaction with the Galactic tidal field. Yet, when the LF is measured near the half-mass radius [i.e., within $(1-3) \times r_{\text{hm}}$] as for all the clusters above including ω Cen, and barring extreme cases of tidal stripping such as those resulting from clusters venturing very close to the Galactic bulge, one should expect only minimal deviations from the original distribution of masses as De Marchi & Paresce (1996, 1997)

have shown observationally and as Richer et al. (1991) had predicted.

If the results of Elson et al. were confirmed, however, they could modify this picture. In fact, because ω Cen is both too massive to have undergone serious internal dynamical modifications in a Hubble time and is sufficiently far from the Galactic plane and bulge not to have experienced major tidal stripping (see Dauphole et al. 1996), its LF should reflect the IMF much more closely than any of the LFs of the other clusters listed above. Since clusters with a similar metallicity are expected to form with a similar IMF, the discrepancy between the LF of ω Cen and that of the other clusters would seem to suggest that GCs are born with a steeply rising IMF that is substantially modified in less massive clusters by dynamical evolution throughout the cluster's lifetime. Thus, in these cases the observed MF no longer corresponds to the IMF.

Such a conclusion would call for a reinterpretation of most of the recent studies based on *Hubble Space Telescope* (*HST*) observations of stellar populations in GCs and in the field that today all point to a deficiency of low-mass stars in the IMF. The implications that such a result could bear on the origin and nature of the dark matter in the Galaxy and the star formation mechanism are so important that we must be able to ensure that the apparent anomaly of the LF of ω Cen reported by Elson et al. is not due to the data reduction process or to the limitation of the data themselves. Most of the conclusions of Elson et al. are based on the analysis of a deep *I*-band image, so that their LF is constructed using little or no color information for MS stars. This is somewhat worrisome, as there are many examples of GC LFs based on single-filter photometry (e.g., Fahlman et al. 1989; Richer et al. 1991) that subsequently have proved to be incorrect at the faint end, although in these cases the error might have originated mostly because of crowding.

To better understand this issue, I have used a larger set of Wide Field Planetary Camera 2 (WFPC2) images of ω Cen now available from the *HST* archive and have subjected

¹ Based on observations with the NASA/ESA *Hubble Space Telescope*, obtained at the Space Telescope Science Institute, which is operated by the Association of Universities for Research in Astronomy, Inc., under NASA contract NAS 5-26555.

these data to exactly the same processing that I adopted for all other clusters studied so far. In this paper, I describe the LF obtained in this way and compare it with those of other GCs observed with the same instrumentation, as well as with the near-IR LF recently obtained with the Near-Infrared Camera and Multi-object Spectrograph (NICMOS) for the same object (Pulone et al. 1998).

2. DATA

The data discussed in this paper have been obtained with WFPC2 on board *HST* using the F606W and F814W filters (Biretta 1996). Two fields have been observed: the first, located $\sim 7'$ southwest of the cluster center, was imaged on 1994 August 29 with a total exposure time of 1800 s in the F606W band and 2800 s in the F814W filter, while the second, located ~ 4.6 southeast of the center, was observed on 1995 June 4 with a total exposure time of 3000 s in F606W and 4600 s in F814W. The images of the first field are the same as those described in the Elson et al. paper (their field 2), although they erroneously quote for it a distance of 17.4 from the cluster center. The analysis described here has been limited only to the PC chips in both fields, as the high stellar density makes it difficult to obtain accurate photometry for faint stars in the WF chips because of their larger plate scale (0.1 pixel^{-1} vs. 0.043 pixel^{-1}), thus increasing the uncertainty on the derived LF. The two PC fields used in this paper are shown in Figure 1.

After standard *HST* WFPC2 pipeline processing, including frame registration and cosmic-ray rejection, stellar fluxes have been measured using the core aperture photometry technique (De Marchi et al. 1993) with the same selection of parameters that I used in previous investigations of other clusters with the same instrumentation (see Paresce et

al. 1995 and De Marchi & Paresce 1995 for a detailed description of our photometric analysis and for a discussion of the current uncertainties in the reduction and calibration of WFPC2 photometric data).

With a detection threshold conservatively set at 5σ above the local average background in the PSF peak, I have selected a total of 1070 stars in field 1 with well-defined fluxes in both bands. In field 2, because of the presence of three very bright stars, photometry has been restricted to the bottom right portion of the image (see Fig. 1), where I have found 830 objects satisfying the detection criterion above in both filters.

Instrumental magnitudes have been converted into the WFPC2 ground system by using the photometric calibration prescriptions for the WFPC2 (Holtzman et al. 1995). These have been used to construct color-magnitude diagrams (CMDs) extending down to $m_{814} \simeq 25$, as shown in Figure 2. The internal accuracy of the photometry varies in both fields from a few hundredths of a magnitude for bright, unsaturated stars at $m_{814} \simeq 19$ to ~ 0.1 mag at $m_{814} \simeq 24$, but the photometry in field 2 is consistently noisier than in field 1 because of crowding, which makes background determination more uncertain in a denser environment (the number of stars per unit area is more than 3 times larger in field 2). This effect can be seen by comparing the “width” of the MS in both fields and noticing that the MS in field 1 is narrower than the other at any given magnitude. The MS of ω Cen is truncated at the bright end because of saturation, setting in at $m_{814} \simeq 17$ in field 1 and $m_{814} \simeq 19$ in field 2 owing to the different exposure duration.

From the CMDs of Figure 2 and adopting the 2.5σ clipping criterion described in De Marchi & Paresce (1995),

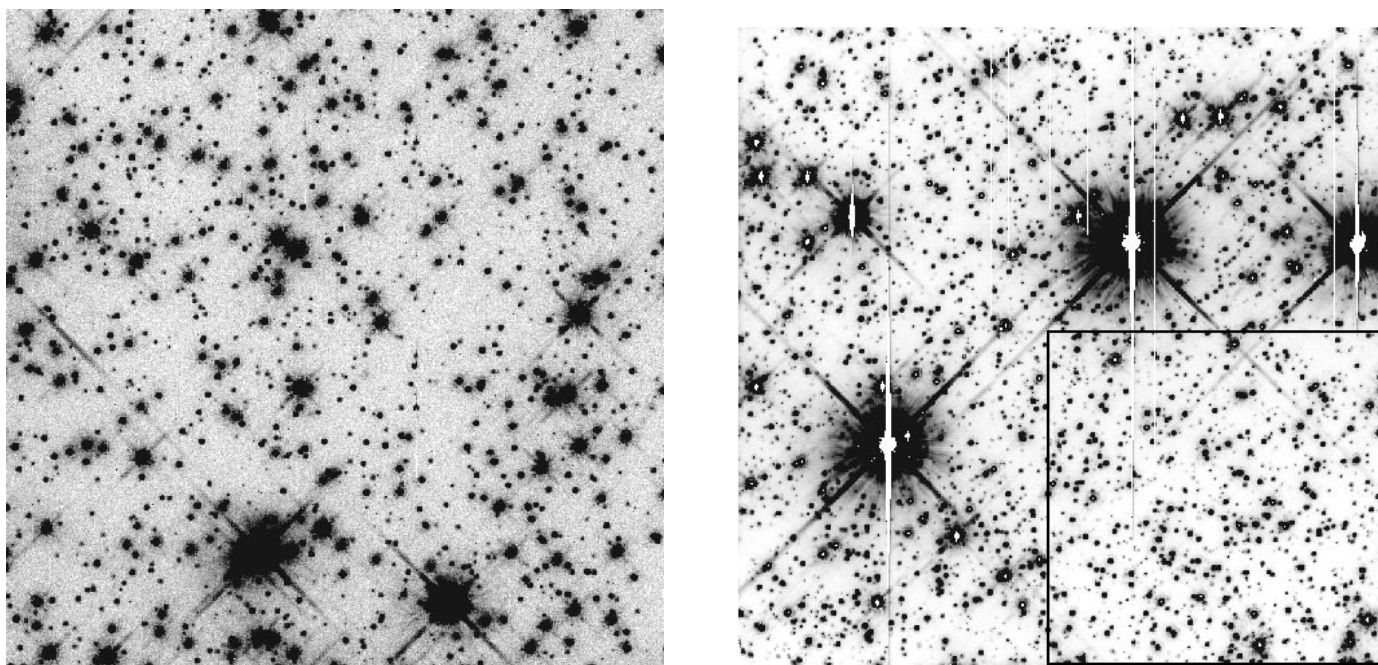


FIG. 1.—*Left*: Negative image of a region $\sim 30' \times 30'$ located $\sim 7'$ southwest of the center of ω Cen as seen through the F814W filter of WFPC2 (PC chip) with an exposure of 1800 s duration (field 1). *Right*: Negative image of a region $\sim 30' \times 30'$ located ~ 4.6 southeast of the center of ω Cen observed with the F814W filter of the WFPC2 (PC chip) with an exposure of 4600 s duration (field 2); the box in the bottom right corner marks the region in which photometry was carried out.

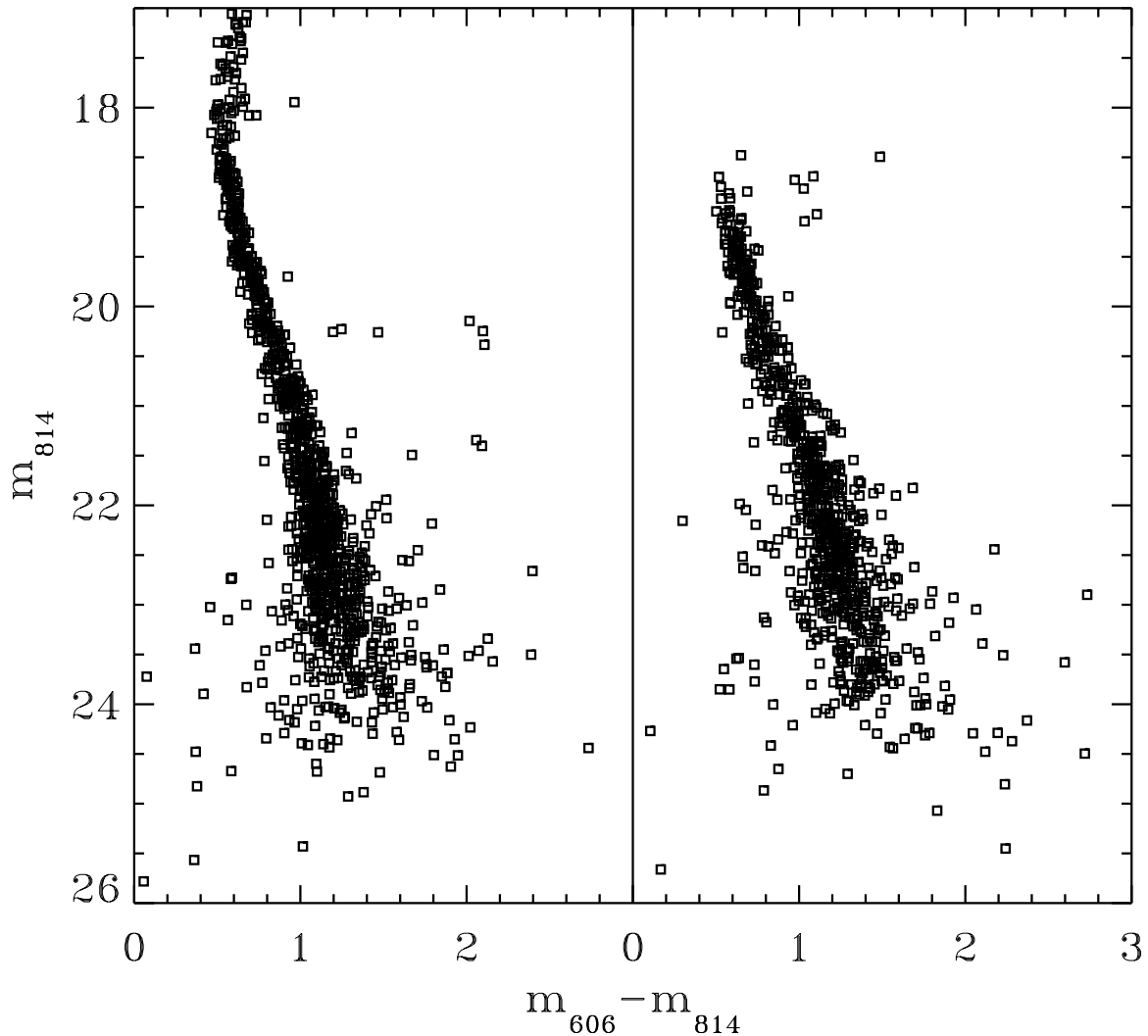


FIG. 2.—CMDs of the stars in field 1 (left) and field 2 (right). The MS in field 2 is truncated above $m_{814} \approx 18.5$ because of saturation.

I have measured the LF of MS stars by counting the number of objects in each 0.5 mag bin along the m_{814} axis and within ± 2.5 times the $m_{606} - m_{814}$ color standard deviation around the MS ridgeline. The contamination due to field stars was removed by counting the number of objects falling outside of the quoted $\pm 2.5 \sigma$ belt but still within the color range $0.5 < m_{606} - m_{814} < 3$. This number has been scaled by the effective color range ($2.5\text{--}5 \sigma$ mag), multiplied by the “width” of the MS belt (i.e., 5σ mag) to determine the expected number of field stars falling within the cluster MS, and finally subtracted from the MS star counts. The selection of the above color limits stems from the working assumption that field objects fill almost uniformly the quoted range. The density of objects on both sides of the MS in Figure 2 is rather low, in agreement with theoretical expectations (Méndez & Van Altena 1996). It is, therefore, unlikely that we are underestimating the number of stars in the MS due to field contamination (see also Elson et al. on this issue).

A reliable determination of the LF from the CMDs of Figure 2 requires the assessment of the degree of photometric incompleteness as a function of the magnitude. I

have, therefore, run a number of trials by adding artificial stars to the individual frames and then combined and reduced them again with the same parameters used in the scientific investigation (see De Marchi & Paresce 1995 for more details). In this way, I have determined that photometry in field 1 is $\sim 100\%$ complete down to $m_{814} \approx 22.5$ and that the completeness decreases to $\sim 85\%$ at $m_{814} \approx 24$ because of crowding. Field 2 is more crowded, and photometric completeness is $\sim 100\%$ for stars brighter than $m_{814} \approx 20$, dropping to $\sim 50\%$ at $m_{814} \approx 24$.

3. DISCUSSION AND CONCLUSIONS

The LFs measured in this way and corrected for photometric incompleteness are shown in Figure 3, where data from fields 1 and 2 are indicated with squares and circles, respectively. I have applied a vertical offset of 0.1 dex to the field 2 data to account for the different stellar density in the two images. In addition, I have used different binning for the data in field 1 and field 2: the size of the m_{814} magnitude bin is the same (0.5 mag) for both fields, but the centers of the bins are displaced by 0.2 mag from each other. In this way, when the LFs are combined in the same graph (Fig. 3)

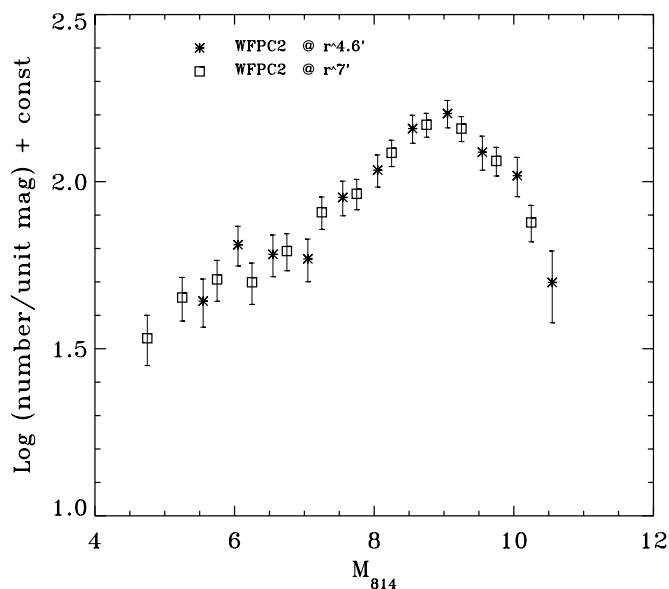


FIG. 3.—Luminosity functions of ω Cen measured in Field 1 (squares) and Field 2 (crosses) using the CMDs of Fig. 2. The centers of the bins used to count stars along the MS in the two fields are displaced by 0.2 mag from each other to provide a finer sampling of the magnitude range.

they provide a finer sampling of the magnitude range. Absolute magnitudes in Figure 3 have been obtained by adopting for ω Cen a distance modulus of $(m - M)_0 = 13.45$ and a color excess of $E(B - V) = 0.15$ (Djorgovski 1993), thus implying $(m - M)_I = 13.7$. The LFs are in excellent agreement with each other within the statistical errors over a range of more than 5 mag, thus indicating that both fields are sampling the same stellar population.

The shape of our LFs, however, differs substantially from that derived by Elson et al. in that those presented here reach a peak at $M_I \simeq 9$ and then clearly drop all the way to the detection limit, well before photometric incompleteness becomes significant and regardless of whether the field at 4.6 or the one at 7' from the center is considered. This behavior is perfectly consistent with that observed in all the other low-metallicity GCs studied so far with the WFPC2 (see references in § 1). To confirm this, in Figure 4 I compare the LFs derived here with the deepest one currently available for a low-metallicity GC, namely, that of NGC 6397, as measured by Paresce et al. (1995) and arbitrarily normalized along the vertical axis. In spite of a small difference in the metal content of the two clusters ($[\text{Fe}/\text{H}] = -1.59$ for ω Cen and $[\text{Fe}/\text{H}] = -1.91$ for NGC 6397; Djorgovski 1993), their LFs agree very well with each other within the observational uncertainties. This is not surprising, as both clusters were imaged near their half-mass radius ($r_{\text{hm}} = 4.8$ for ω Cen; Djorgovski 1993) where the LF should directly reflect the IMF, as the local stellar population is expected to be rather insensitive to dynamical modifications (Richer et al. 1991; De Marchi & Paresce 1997).

Pulone et al. (1998) have recently observed with NICMOS on board the *HST* a region located $\sim 7'$ southwest of the cluster center and have derived a LF for MS stars extending down to $H \simeq 22.5$ ($m_{160} \simeq 26$ in the STMAG magnitude system), corresponding to a mass of $\sim 0.2 M_\odot$. I have converted this LF from the H to the I band using the theoretical mass-luminosity relation calcu-

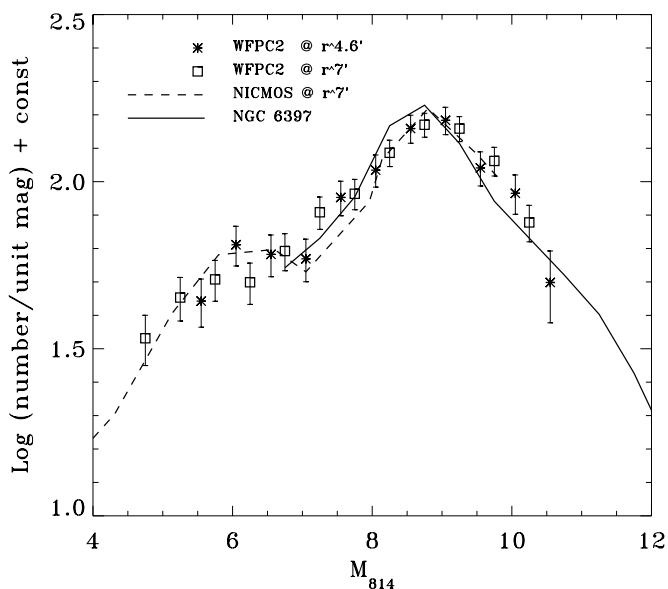


FIG. 4.—The LFs of Fig. 3 are here compared with the LF of the same cluster measured with NICMOS (dashed line) and converted to the F555W, F814W plane, as well as with the I -band LF of NGC 6397.

lated by Baraffe et al. (1997) for the metallicity of ω Cen, as their models of stellar atmospheres reproduce quite accurately the lower portion of the MS of low-metallicity GCs (Chabrier & Méra 1997). The shape of the I -band LF obtained in this way (Fig. 4, dashed line) is in excellent agreement with those measured in the WFPC2 images over the whole magnitude range spanned by both instruments.

It remains difficult to understand the discrepancy between the results presented here and those published by Elson et al. for their innermost field, unless the flattening that they measure at low masses is an artifact due to data processing and, particularly, to the lack of correction for field star and galaxy contamination. On the contrary, the color information contained in the CMD that I use here should make the discrimination between cluster and field objects more robust at the faint end where field stars and faint unresolved galaxies begin to outnumber cluster objects. Although it would be possible to use a model of the Galaxy to estimate and correct for field star contamination, the presence of unresolved galaxies and quasi-stellar objects at $I \simeq 23.5$ and beyond (see, e.g., Flynn, Gould, & Bahcall 1996) can cause large uncertainties.

In conclusion, my results strengthen the scenario suggested by De Marchi & Paresce (1996, 1997) that in order for all the low-metallicity GCs observed so far near the half-mass radius to show very similar LFs at low masses, they have to be born with the same IMF, which is now directly reflected in the LF itself with negligible modifications induced by dynamical evolution. This proves that it is possible to determine the IMF of GC stars, provided that a reliable $M-L$ relation is available and that the LF is measured near the half-mass radius.

I would like to thank Francesco Paresce for many useful discussions on the issues addressed in this paper, and France Allard and Isabelle Baraffe for providing their mass-luminosity relations for low-mass stars.

REFERENCES

- Baraffe, I., Chabrier, G., Allard, F., & Hauschildt, P. 1997, *A&A*, 327, 1054
- Biretta, J., et al. 1996, *Wide Field and Planetary Camera 2 Instrument Handbook* (version 4.0; Baltimore: STScI)
- Chabrier, G., & Méra, D. 1997, *A&A*, 328, 83
- Cool, A., Piotto, G., & King, I. 1996, *ApJ*, 468, 655
- Dauphole, B., Geffret, M., Colin, J., Ducourant, C., Odenkirchen, M., & Tucholke, J. 1996, *A&A*, 313, 119
- De Marchi, G., Nota, A., Leitherer, C., Ragazzoni, R., & Barbieri, C. 1993, *ApJ*, 419, 658
- De Marchi, G., & Paresce, F. 1995, *A&A*, 304, 202
- . 1996, in *Science with the Hubble Space Telescope—II*, ed. P. Benvenuti, D. Macchetto, & E. Schreier (Baltimore: STScI), 310
- . 1997, *ApJ*, 476, L19
- Djorgovski, S. 1993, in *ASP Conf. Ser. 50, Structure and Dynamics of Globular Clusters*, ed. S. Djorgovski & G. Meylan (San Francisco: ASP), 273
- Elson, R., Gilmore, G., Santiago, B., & Casertano, S. 1995, *AJ*, 110, 682
- Fahlman, G., Richer, H., Searle, I., & Thompson, I. 1989, *ApJ*, 343, L49
- Flynn, C., Gould, A., & Bahcall, J. 1996, *ApJ*, 466, L55
- Holtzman, J., Burrows, C., Casertano, S., Hester, J., Trauger, J., Watson, A., & Worthey, G. 1995, *PASP*, 107, 1065
- Méndez, R., & van Alena, W. 1996, *AJ*, 112, 655
- Meylan, G. 1987, *A&A*, 184, 144
- Paresce, F., De Marchi, G., & Romaniello, M. 1995, *ApJ*, 440, 216
- Piotto, G., Cool, A., & King, I. 1997, *AJ*, 113, 1345
- Pulone, L., De Marchi, G., Paresce, F., & Allard, F. 1998, *ApJ*, 492, L41
- Richer, H., Fahlman, G., Buonanno, R., Fusi Pecci, F., Searle, I., & Thompson, I. 1991, *ApJ*, 381, 147